State boundary surface of a hypoplastic model for clays

David Mašín

(corresponding author)
Charles University
Institute of Hydrogeology, Engineering Geology and Applied Geophysics
Albertov 6
12843 Prague 2, Czech Republic
E-mail: masin@natur.cuni.cz
Tel: +420-2-2195 1552, Fax: +420-2-2195 1556

Ivo Herle

Technische Universität Dresden
Institute of Geotechnical Engineering
D-01062 Dresden, Germany
E-mail: ivo.herle@mailbox.tu-dresden.de
Tel: +49-351-46337540 Fax: +49-351-46334131

21st October 2005

Preprint - accepted for
Computers and Geotechnics

Abstract

The paper studies some consequences of the mathematical formulation of the recently proposed hypoplastic model for clays. Particular attention is paid to the question if the hypoplastic model predicts existence of the state boundary surface, defined as a boundary of all admissible states in the stress-void ratio space. It is shown that the model enables us to derive an explicit formulation of asymptotic (swept-out-memory) states in the stress-void ratio space, which constitute so-called swept-out-memory surface. Further it is demonstrated that the swept-out-memory surface is a close approximation of the state boundary surface although, in general, they do not coincide. Finally, the influence of constitutive parameters on the shape of the swept-out-memory surface is studied. For parameters reasonable for fine-grained soils its shape is similar to the state boundary surface of the Modified Cam clay model.

1 Introduction

Hypoplastic constitutive models have been developed since 1980's and since then they have established a solid base for an alternative description of the soil behaviour, without an explicit definition of yield and potential surfaces – see for example the review [34]. Recent hypoplastic models [12, 37] include the concept of critical states and have been successfully used in many computations of boundary value problems within coarse-grained soils, e.g. [36, 28, 17, 24, 8]. The progress of hypoplastic models suitable for the description of fine-grained soils has been delayed. Rate-dependent [26, 13] and rate-independent [15, 21] hypoplastic models for clays promise to follow the success of the development for sand. Nevertheless, a thorough testing of various constitutive aspects is required in order to ensure a correct performance in general conditions of boundary value problems.

One of the key characteristics of the behaviour of fine-grained soils, incorporated in different ways in most of the currently available elasto-plastic constitutive models for fine-grained soils, is a surface in the stress-void ratio space which bounds all admissible states (state boundary surface, SBS). As hypoplastic models do not incorporate the state boundary surface explicitly, the primary aim of this paper is to investigate if these models (in particular a hypoplastic model for clays [21]) predict the state boundary surface as a by-product of the constitutive formulation.

In this paper hypoplastic models will be distinguished according to the terminology laid out by Kolymbas [19]. Models without internal structure (*i.e.* with Cauchy stress tensor $\mathbf{T}$ being the only state variable) will be referred to as *amorphous*, whereas models with internal structure (incorporated by means of additional state variables) *endomorphous*. In this work we restrict our attention to *endomorphous* models with a single additional state variable (void ratio e). Solid mechanics sign convention (compression negative) will be adopted throughout, all stresses are considered as effective in the sense of Terzaghi. The operator

arrow is defined as $\vec{\mathbf{X}} = \mathbf{X}/\|\mathbf{X}\|$, trace by $\operatorname{tr}\mathbf{X} = \mathbf{X} : \mathbf{1}$, with $\mathbf{1}$ being the second-order unit tensor. $\hat{\mathbf{T}}$ is the normalised stress defined by $\hat{\mathbf{T}} = \mathbf{T}/\operatorname{tr}\mathbf{T}$, $\|\mathbf{D}\| = \sqrt{\mathbf{D} : \mathbf{D}}$ is the Euclidian norm of $\mathbf{D}$, which stands for the Euler's stretching tensor.

The paper starts by introducing proportional response envelopes and definition of asymptotic (swept-out-memory) states. Thereafter, pointing to the analogy with the limit and bounding surfaces of *amorphous* hypoplastic models, a mathematical formulation of the surface in the stress-void ratio space which covers all asymptotic states (named *swept-out-memory* surface) is developed. Further, using the concept of so-called normalised incremental stress response envelopes, it is demonstrated that swept-out-memory surface is a close approximation of the state boundary surface. Finally, the influence of model parameters on the shape of the swept-out-memory surface is discussed.

2 Response envelopes and swept-out-memory states

Response envelopes in axisymmetric stress space [10] were proposed as a graphical representation of resulting stress rates imposed by different unit strain rates $\sqrt{D_a^2 + 2D_r^2} = 1$ at one particular initial state (D_a and D_r being axial and radial strain rates, respectively). This concept proved to be useful in studying properties of rate-type constitutive equations, however due to the infinitesimal nature of stress and strain rates they can not be studied experimentally. Hypoplastic models yield elliptic (smooth) response envelopes, whereas elasto-plastic models are characterised by non-smooth envelopes.

A modification of the stress-rate envelopes towards *incremental stress response envelopes*, as defined in [35], may be applied for finite values of stress and strain increments. Linear strain paths with a fixed direction of stretching $\vec{\mathbf{D}}$ and with a fixed length $R_{\Delta\epsilon}$ (Eq. (2)) yield the stress response $\Delta\mathbf{T}$ in the stress space $\mathbf{T}$ (see Fig. 1 for axisymmetric conditions). The stress increment $\Delta\mathbf{T}$ may be calculated by the time integration of the rate form of the constitutive equation:

$$\Delta\mathbf{T} = \int_{t_0}^{t_1} \mathring{\mathbf{T}} dt \tag{1}$$

where $\mathring{\mathbf{T}}$ stands for a co-rotated (Jaumann) stress rate. The shape and size of the incremental stress response envelopes depends on the value of

$$R_{\Delta\epsilon} = \| \int_{t_0}^{t_1} \mathbf{D}\, dt \| \tag{2}$$

An inverse procedure with constant $\vec{\mathring{\mathbf{T}}}$ and fixed length stress increments $R_{\Delta\sigma}$, constituting in the strain space *incremental strain response envelopes*, was applied experimentally by Royis and Doanh [30] for sand and Costanzo et al. [6] for clays. These results were followed

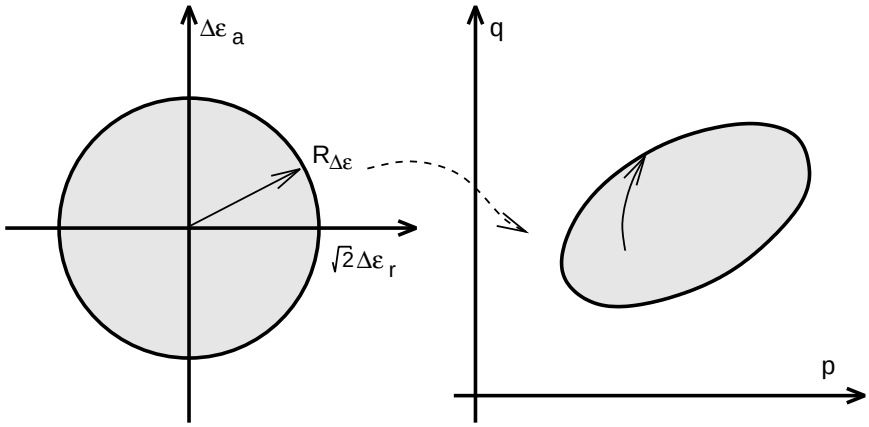

Figure 1: On the definition of the *incremental stress response envelope* for the special case of axisymmetric conditions

by numerical investigations using DEM with rigid spheres [3] and used for evaluation of predictive capabilities of different constitutive models [23, 33].

In addition to incremental responses, constitutive models should predict so-called asymptotic states, as pointed out by Kolymbas [18]. Stress paths of sound constitutive models should tend to proportional stress paths (constant $\vec{\mathbf{T}}$) for sufficiently long proportional strain paths (constant $\vec{\mathbf{D}}$). As corresponding $\vec{\mathbf{T}}$ and $\vec{\mathbf{D}}$ at asymptotic states are independent of the initial state, these states are often denoted as swept-out-memory (SOM) states [14], and may be seen as *attractors* of the soil behaviour [11] (see Fig. 2).

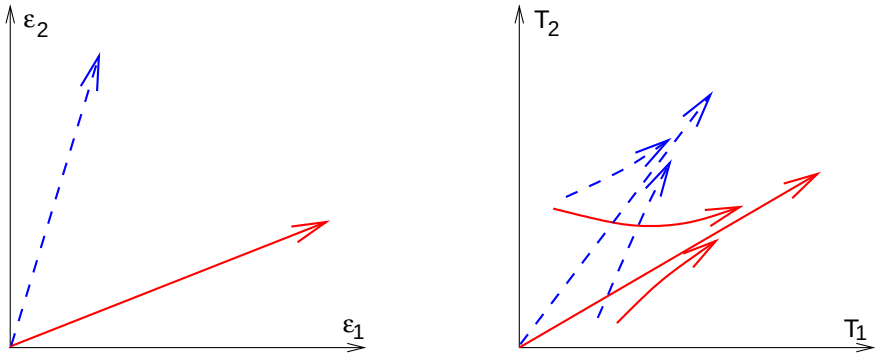

Figure 2: SOM-behaviour: proportional stress paths for proportional strain paths

The concept of swept-out-memory states may be extended also to *endomorphous* constitutive models. For pairs of proportional stress and strain paths one can find corresponding void ratios e_p dependent on the mean stress $p = -\operatorname{tr}\mathbf{T}/3$ (Fig. 3). Combinations of e_p and p plotted in the $e : p$ space are usually denoted as normal compression lines (NCL). A particular example of SOM-states is the critical state with $\operatorname{tr}\mathbf{D} = 0$ and $\mathring{\mathbf{T}} = \mathbf{0}$, where SOM

stress ratio follows from the critical state friction angle φ_c and void ratio from the position of the critical state line in the stress-void ratio space.

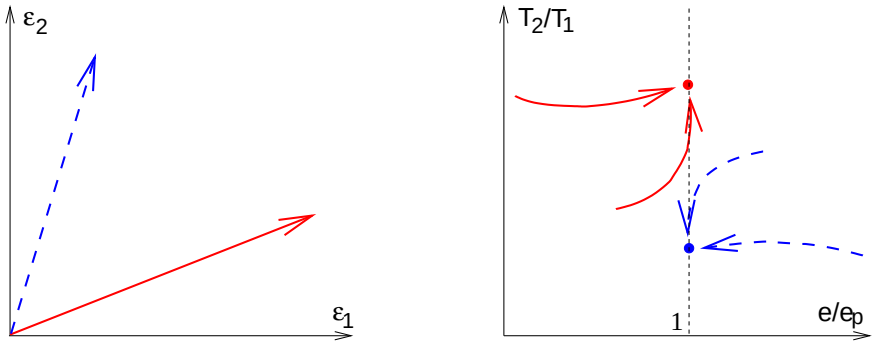

Figure 3: Extended SOM-behaviour including void ratio

3 Basic properties of the considered constitutive model

This paper focuses on the particular hypoplastic model for clays [21], whose complete mathematical formulation is given in Appendix A. The model may be written in its most general form by

$$\mathring{\mathbf{T}} = \boldsymbol{h}\left(\mathbf{T}, \mathbf{D}, e\right) \tag{3}$$

The model belongs to the sub-class of hypoplastic models referred to as *endomorphous* (Sec. 1). The particular form of the isotropic tensor-valued function $\boldsymbol{h}$ follows from [12] and reads

$$\mathring{\mathbf{T}}\left(\mathbf{T}, \mathbf{D}, e\right) = f_s\left(\operatorname{tr}\mathbf{T}\right)\left[\boldsymbol{\mathcal{L}}(\hat{\mathbf{T}}) : \mathbf{D} + f_d\left(\operatorname{tr}\mathbf{T}, e\right)\mathbf{N}(\hat{\mathbf{T}})\|\mathbf{D}\|\right] \tag{4}$$

where f_s and f_d are so-called *barotropy* and *pyknotropy* factors [12], which incorporate the influence of the mean stress and void ratio. Note that differently from [12], the barotropy factor f_s of the hypoplastic model for clays is independent of void ratio e.

The following properties of the considered constitutive equation are important for the developments presented in this paper:

1. The function $\boldsymbol{h}$ is positively homogeneous of degree 1 in $\mathbf{D}$:

$$\boldsymbol{h}\left(\mathbf{T}, \gamma\mathbf{D}, e\right) = \gamma\boldsymbol{h}\left(\mathbf{T}, \mathbf{D}, e\right) \tag{5}$$

   for any $\gamma > 0$. This property implies that the behaviour of the material is not influenced by any change in the time scale, i.e. the behaviour is rate-independent.

2. For a constant value of the *pyknotropy* factor f_d, the function $\boldsymbol{h}$ is positively homogeneous of *degree 1* in $\mathbf{T}$, thus

$$\boldsymbol{h}\left(\gamma\mathbf{T},\mathbf{D},e\right)=\gamma\boldsymbol{h}\left(\mathbf{T},\mathbf{D},e\right) \tag{6}$$

for any $\gamma>0$. This property follows from the fact that in the considered model the tensors $\boldsymbol{\mathcal{L}}$ and $\mathbf{N}$ are functions of the normalised stress $\hat{\mathbf{T}}$ only, and the ratio $f_s/\operatorname{tr}\mathbf{T}$ is constant (consequence of the assumption of a linear isotropic normal compression line in the $\ln(1+e)$:$\ln p$ space [2]).

For cases described by Eq. (6), the behaviour may be normalised by the current mean stress p, or in a general case, by Hvorslev's equivalent pressure on the isotropic normal compression line p_e^*. This procedure will be applied in Sec. 5.

3. The model predicts swept-out-memory states, introduced in Sec. 2. For a discussion on the prediction of SOM behaviour by hypoplastic models the reader is referred to [27].

Before proceeding to the derivation of the state boundary surface of the considered constitutive model, we recall some basic properties of more simple *amorphous* hypoplastic models.

4 Limit surface and Bounding surface

Amorphous hypoplastic constitutive models (e.g. model from [38]) may still be written using Eq. (4) [20], considering $f_d=\text{const}$. Eq. (3) therefore reduces to

$$\mathring{\mathbf{T}}=\boldsymbol{h}\left(\mathbf{T},\mathbf{D}\right) \tag{7}$$

For brevity, we will consider the factor f_s in Eq. (4) embedded in the constitutive tensors $\boldsymbol{\mathcal{L}}$ and $\mathbf{N}$. Therefore, we may write

$$\mathring{\mathbf{T}}\left(\mathbf{T},\mathbf{D}\right)=\boldsymbol{\mathcal{L}}(\mathbf{T}):\mathbf{D}+\mathbf{N}(\mathbf{T})\|\mathbf{D}\| \tag{8}$$

Based on the fundamental experimental evidence, all reasonable constitutive models for soils must consider the domain of admissible states in the *stress space*, bounded by a surface, formally defined through an isotropic tensor function. In the sequel, we will distinguish between two different notions: *limit surface* and *bounding surface*:

1. *Limit surface* [5] $f(\mathbf{T})$, sometimes referred to as invertibility surface [34], failure surface [39] or yield surface [19], is defined in the *stress* space as a boundary of all states where Eq. (7) is invertible.

2. *Bounding surface* [27] $b(\mathbf{T})$ (or bound surface [39]) is defined in the *stress* space as a boundary of all admissible states.[1]

Limit surface has been embedded even in very early versions of hypoplastic models (see, e.g., [18]) as a by-product of a particular choice of tensorial constitutive functions. It has been however soon recognised that the mathematical structure of Eq. (8) allows us to define the limit surface explicitly (e.g., [4, 1, 37]).

Following [34], Eq. (8) may be written as

$$\gamma\mathbf{S} = \boldsymbol{\mathcal{L}} : \mathbf{D} + \mathbf{N}\|\mathbf{D}\| \tag{9}$$

with γ being the norm of the stress increment $\gamma = \|\mathring{\mathbf{T}}\|$ and $\mathbf{S}$ its direction $\mathbf{S} = \vec{\mathring{\mathbf{T}}}$. Due to the Property 1. of Sec. 3 we may, without loss of generality, assume $\|\mathbf{D}\| = 1$. Eq. (9) then reads

$$\gamma\mathbf{S} = \boldsymbol{\mathcal{L}} : \vec{\mathbf{D}} + \mathbf{N} = \boldsymbol{\mathcal{L}} : (\vec{\mathbf{D}} + \mathbf{B}) \tag{10}$$

with

$$\mathbf{B} = \boldsymbol{\mathcal{L}}^{-1} : \mathbf{N} \tag{11}$$

Expressing (11) obviously requires invertibility of the tensor $\boldsymbol{\mathcal{L}}$ of the particular *amorphous* hypoplastic model.

From Eq. (10) we get

$$\vec{\mathbf{D}} = \gamma\boldsymbol{\mathcal{L}}^{-1} : \mathbf{S} - \mathbf{B} \tag{12}$$

Because $\|\vec{\mathbf{D}}\| = 1$, we have

$$1 = \|\gamma\boldsymbol{\mathcal{L}}^{-1} : \mathbf{S} - \mathbf{B}\| \tag{13}$$

and therefore

$$\gamma^2\|\boldsymbol{\mathcal{L}}^{-1} : \mathbf{S}\|^2 - 2\gamma(\boldsymbol{\mathcal{L}}^{-1} : \mathbf{S}) : \mathbf{B} + \|\mathbf{B}\|^2 - 1 = 0 \tag{14}$$

For states inside the limit surface we require that Eq. (14) has a single real positive solution for the norm of the stress increment γ. It may be shown from the requirement

$$(\boldsymbol{\mathcal{L}}^{-1} : \mathbf{S}) : \mathbf{B} < \sqrt{[(\boldsymbol{\mathcal{L}}^{-1} : \mathbf{S}) : \mathbf{B}]^2 - \|\boldsymbol{\mathcal{L}}^{-1} : \mathbf{S}\|^2(\|\mathbf{B}\|^2 - 1)} \tag{15}$$

that this condition is satisfied for

$$\|\mathbf{B}\|^2 - 1 < 0 \tag{16}$$

Equation

$$\|\mathbf{B}\|^2 - 1 = 0 \tag{17}$$

[1] Note that this definition is different compared to the one usually adopted for bounding surface plasticity models [9] and kinematic hardening elasto-plastic models (e.g., [32]), where the term bounding surface is used for the intersection of the state boundary surface and an elastic wall.

therefore describes the limit of invertibility of Eq. (8) and, according to its definition, the limit surface[2]. The fact that one solution corresponds to $\gamma = 0$ may be represented graphically using the concept of response envelopes (Sec. 2). As may be seen from Fig. 4, the reference stress point is then located on the response envelope. For states outside the limit surface the solution of Eq. (14) is not unique and the reference stress point is located outside the response envelope.

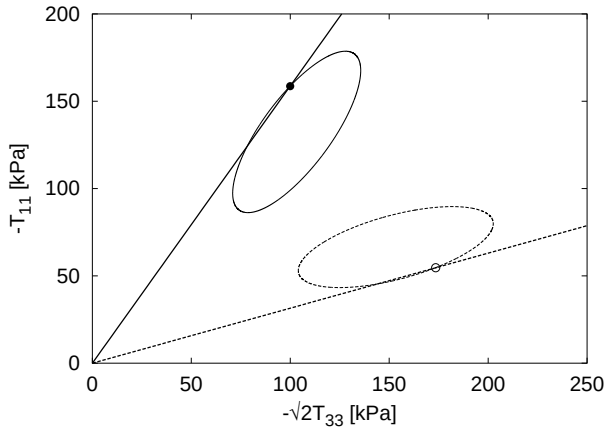

Figure 4: Stress rate response envelopes for the initial stress located on the limit surface

An investigation of Fig. 4 reveals that the limit surface $f(\mathbf{T})$ does not coincide with the bounding surface $b(\mathbf{T})$: for some directions of stretching the corresponding stress rates surpass $f(\mathbf{T})$. This fact, which was already described for example in [39], is a common feature of hypoplastic models developed at the University of Karlsruhe (see [34]) and is related to the derivation of constitutive tensors $\boldsymbol{\mathcal{L}}$ and $\mathbf{N}$. As noticed by [39] and as may be appreciated also from Fig. 4, however, the difference between the bounding and limit surfaces is not significant from the point of view of parameter identification.

The bounding surface can be mathematically characterised also by Eq. (14) requiring the magnitude of the stress rate $\gamma \geq 0$. Inserting the condition of the *limit surface* ($\|\mathbf{B}\|^2 - 1 = 0$) into Eq. (14) yields

$$\gamma^2 \|\boldsymbol{\mathcal{L}}^{-1} : \mathbf{S}\|^2 - 2\gamma(\boldsymbol{\mathcal{L}}^{-1} : \mathbf{S}) : \mathbf{B} = 0 \tag{18}$$

which leads to inequality constraining the possible directions of the stress rate $\mathbf{S}$:

$$(\boldsymbol{\mathcal{L}}^{-1} : \mathbf{S}) : \mathbf{B} > 0 \tag{19}$$

The bounding surface thus follows [34] from the condition

$$(\boldsymbol{\mathcal{L}}^{-1} : \mathbf{S}) : \mathbf{B} = 0 \tag{20}$$

[2]Eqs. (10)–(17) are useful for the subsequent comparison of the limit and bounding surfaces. Limit surface may be also found directly from $\mathring{\mathbf{T}} = 0$ following, e.g., [39]. In that case $\mathbf{0} = \boldsymbol{\mathcal{L}} : (\mathbf{D} + \mathbf{B}\|\mathbf{D}\|)$, thus $\vec{\mathbf{D}} = -\mathbf{B}$ and $\|\mathbf{B}\| - 1 = 0$ at the limit surface, which corresponds to (17).

As noted above, Eqs. (18)–(20), describing the bounding surface, hold for stress states at the limit surface. They may be therefore used to specify conditions for $b(\mathbf{T})$ to coincide with $f(\mathbf{T})$. As shown in [27], it is possible to enforce coincidence of $b(\mathbf{T})$ and $f(\mathbf{T})$ for hypoplastic models by a suitable rotation of the hypoelastic tensor $\boldsymbol{\mathcal{L}}$. Note also that $b(\mathbf{T}) = f(\mathbf{T})$ is a common feature of all CLoE hypoplastic models [5].

5 Swept-out-memory surface

Let us now consider the case of *endomorphous* hypoplastic models (particularly the model from [21]) with the rate-formulation given in Eq. (4). For these models, the definitions of the limit and bounding surfaces in the *stress* space are not unique, as both depend on the additional scalar state variable, void ratio e. Based on the experimental evidence, which led in 1960's to the development of the critical state soil mechanics in Cambridge [29, 31], the constitutive model should describe a single surface in the stress-void ratio space, which bounds all admissible states. This surface is traditionally called *state boundary surface* (SBS). It is, in general, a surface in the four-dimensional space of the three principal components of the stress tensor $\mathbf{T}$ and void ratio e.

The property 2. from Sec. 3 allows us to simplify the following developments by introducing a normalisation factor taking into account both changes of void ratio and of mean pressure. A suitable quantity is Hvorslev's equivalent pressure p_e^* at the isotropic normal compression line (see Fig. 5), following from the formulation of the isotropic NCL:

$$\ln(1+e) = N - \lambda^* \ln\left(\frac{p_e^*}{p_r}\right) \tag{21}$$

with p_r being the reference stress of 1 kPa. Using this normalisation the state boundary surface may be, in general, fully characterised in the three-dimensional space defined by the principal components of the normalised stress tensor $\mathbf{T}_n$, where

$$\mathbf{T}_n = \frac{\mathbf{T}}{p_e^*} \tag{22}$$

The normalised stress rate $\dot{\mathbf{T}}_n$ follows from (22)

$$\dot{\mathbf{T}}_n = \frac{\dot{\mathbf{T}}}{p_e^*} - \frac{\mathbf{T}}{(p_e^*)^2}\dot{p}_e^* \tag{23}$$

The stress rate $\dot{\mathbf{T}}$ is, under the assumption of small strains, given by (4) and the rate of $\dot{p}_e^*$ is found by the time-differentiation of the isotropic NCL given by Eq. (21):

$$\frac{\dot{e}}{1+e} = -\frac{\lambda^*}{p_e^*}\dot{p}_e^* \tag{24}$$

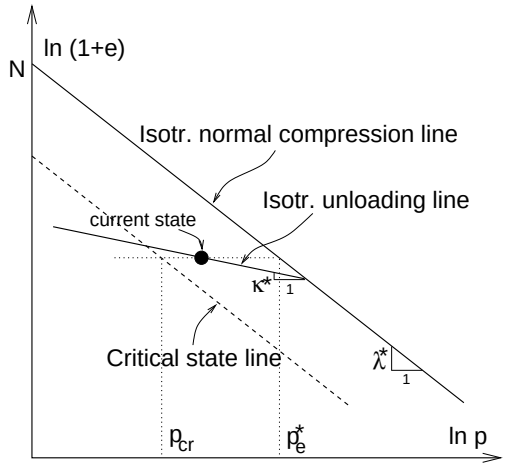

Figure 5: On the definition of Hvorslev's equivalent pressure p_e^*.

From the assumption of grain incompressibility we have

$$\dot{e} = (1+e)\,\mathrm{tr}\,\mathbf{D} \tag{25}$$

and thus

$$\dot{p}_e^* = -\frac{p_e^*}{\lambda^*}\,\mathrm{tr}\,\mathbf{D} \tag{26}$$

Substituting (4) and (26) into (23) we get

$$\dot{\mathbf{T}}_n = \frac{1}{p_e^*}\left(\boldsymbol{\mathcal{L}}\mathbf{D} + f_d\mathbf{N}\|\mathbf{D}\|\right) + \frac{\mathbf{T}\,\mathrm{tr}\,\mathbf{D}}{p_e^*\lambda^*} \tag{27}$$

For brevity, *barotropy* factor f_s has been embedded in the constitutive tensors $\boldsymbol{\mathcal{L}}$ and $\mathbf{N}$.

We first try to find an expression equivalent to the limit surface in the stress-void ratio space. As the limit surface in the *stress* space was defined by $\mathring{\mathbf{T}} = \mathbf{0}$ for one direction of stretching $\vec{\mathbf{D}}$ (Eq. 17), we define its equivalent in the stress-void ratio space by $\dot{\mathbf{T}}_n = \mathbf{0}$. By applying this definition on (27) we get

$$-\frac{\mathbf{T}}{\lambda^*}\,\mathrm{tr}\,\mathbf{D} = \boldsymbol{\mathcal{L}} : \mathbf{D} + f_d\mathbf{N}\|\mathbf{D}\| \tag{28}$$

To solve Eq. (28) for a given $\mathbf{T}$ with unknowns $\vec{\mathbf{D}}$ and f_d, we introduce a fourth order tensor $\boldsymbol{\mathcal{A}}$

$$\boldsymbol{\mathcal{A}} = \boldsymbol{\mathcal{L}} + \frac{1}{\lambda^*}\mathbf{T}\otimes\mathbf{1} \tag{29}$$

such that

$$\boldsymbol{\mathcal{A}} : \vec{\mathbf{D}} = \boldsymbol{\mathcal{L}} : \vec{\mathbf{D}} + \frac{\mathbf{T}}{\lambda^*}\,\mathrm{tr}\,\vec{\mathbf{D}} \tag{30}$$

Eq. (28) may be divided by $\|\mathbf{D}\| \neq \mathbf{0}$ and rewritten

$$\boldsymbol{\mathcal{A}} : \vec{\mathbf{D}} + f_d \mathbf{N} = 0 \tag{31}$$

Since $\|\vec{\mathbf{D}}\| = 1$, we get

$$f_d = \|\boldsymbol{\mathcal{A}}^{-1} : \mathbf{N}\|^{-1} \tag{32}$$

(for invertibility condition of the tensor $\boldsymbol{\mathcal{A}}$ see Appendix B) and

$$\vec{\mathbf{D}} = -\frac{\boldsymbol{\mathcal{A}}^{-1} : \mathbf{N}}{\|\boldsymbol{\mathcal{A}}^{-1} : \mathbf{N}\|} \tag{33}$$

As may be seen from the definitions of tensors $\boldsymbol{\mathcal{A}}$ and $\mathbf{N}$, the quantity $\boldsymbol{\mathcal{A}}^{-1} : \mathbf{N}$, and therefore also $\vec{\mathbf{D}}$ and f_d for $\dot{\mathbf{T}}_n = \mathbf{0}$, are constant for a given $\vec{\mathbf{T}}$. As the condition $\dot{\mathbf{T}}_n = \mathbf{0}$ indeed implies $\vec{\mathbf{T}} = \text{const.}$, Eq. (28) describes asymptotic (swept-out-memory) states as defined in Sec. 2, provided that the evolution equation for f_d is consistent with (28). Therefore, we name the equivalent of the limit surface for the stress-void ratio space a *swept-out-memory (SOM) surface*. From (28) it is also obvious that condition $\operatorname{tr} \mathbf{D} = 0$ directly implies $\mathring{\mathbf{T}} = \mathbf{0}$, so the critical state is predicted as a particular SOM state.

The corresponding response in the $p : e$ space may be found by taking the trace of Eq. (28) and considering $\boldsymbol{\mathcal{L}} : \mathbf{D} + f_d \mathbf{N} \|\mathbf{D}\| = \mathring{\mathbf{T}}$. We get

$$\dot{p} = -\frac{p}{\lambda^*} \operatorname{tr} \mathbf{D} \tag{34}$$

which is the rate formulation of the normal compression line with the slope λ^* in the $\ln(1+e) : \ln p$ space. Positions of different NCLs in this space (and therefore the shape of the SOM surface) are controlled by the *pyknotropy* factor f_d, which in the considered model reads

$$f_d = \left(\frac{2p}{p_e^*}\right)^{\alpha} \tag{35}$$

with α being a constant calculated from the model parameters (see Appendix A) and p_e^* comes from (21). Factor f_d is constant along any line characterised by (34), which ensures consistency between evolution equation for f_d and (28) and thus implies that Eq. (28) describes SOM states.

Combining Eqs. (32) and (35) allows us to calculate the value of p_e^* at the SOM surface at any stress level $\mathbf{T}$ and consequently to find the shape of the SOM surface in the normalised $\mathbf{T}_n$ space:

$$p_e^* = -\frac{2}{3} \operatorname{tr} \mathbf{T} \|\boldsymbol{\mathcal{A}}^{-1} : \mathbf{N}\|^{1/\alpha} \tag{36}$$

The shape of the SOM surface in the normalised triaxial stress space, plotted for triaxial stress invariants $q = -(\mathrm{T}_a - \mathrm{T}_r)$ and p, is shown in Fig. 6 for material parameters given in Tab. 1.

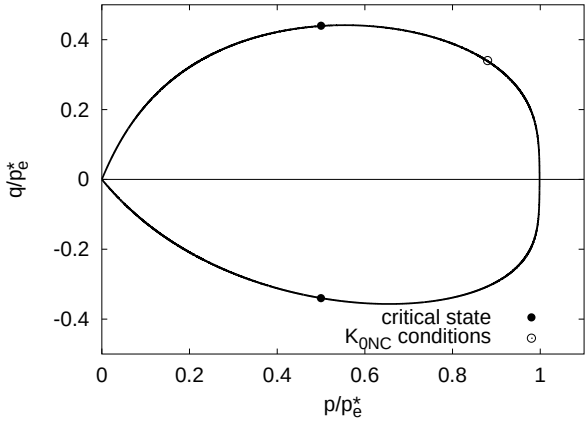

Figure 6: Swept-out-memory surface in the normalised triaxial stress space for the hypoplastic model [21] using London clay parameters (Tab. 1)

6 State boundary surface

In this section we discuss the difference between the swept-out-memory surface, defined in Sec. 5, and the state boundary surface. Without loss of generality we again study response of the considered model in the normalised space $\mathbf{T}_n$. The state boundary surface is defined as an envelope of all admissible states of a soil element. In other words, no outer response in the normalised space $\mathbf{T}_n$ can be generated. Using the concept of response envelopes (Sec. 2), stress rate response envelope plotted in the normalised $\mathbf{T}_n$ space (normalised response envelope, NRE) for the states at the state boundary surface must not cross-sect the surface (i.e., must have a common tangent with the state boundary surface).

We first presume that the state boundary surface is equal to the swept-out-memory surface. A tangent to the normalised response envelope may then be found using a similar procedure to that applied in Sec. 4 for evaluation of bounding surface of *amorphous* hypoplastic models. Let γ_n be the norm of the normalised stress rate $\dot{\mathbf{T}}_n$ ($\gamma_n = \|\dot{\mathbf{T}}_n\|$) and $\mathbf{S}_n$ its direction ($\mathbf{S}_n = \dot{\mathbf{T}}_n/\|\dot{\mathbf{T}}_n\|$). Using the definition of the tensor $\boldsymbol{\mathcal{A}}$ (Eq. 29) and assuming, without loss of generality, $\|\mathbf{D}\| = 1$, Eq. (27) reads

$$p_e^* \gamma_n \mathbf{S}_n = \boldsymbol{\mathcal{A}} : \vec{\mathbf{D}} + f_d \mathbf{N} \tag{37}$$

or

$$p_e^* \gamma_n \mathbf{S}_n = \boldsymbol{\mathcal{A}} : (\vec{\mathbf{D}} + f_d \mathbf{B}_n) \tag{38}$$

with

$$\mathbf{B}_n = \boldsymbol{\mathcal{A}}^{-1} : \mathbf{N} \tag{39}$$

Thus (from (38))

$$\vec{\mathbf{D}} = p_e^* \gamma_n \boldsymbol{\mathcal{A}}^{-1} : \mathbf{S}_n - f_d \mathbf{B}_n \tag{40}$$

taking the norm of (40) we get

$$(p_e^*)^2\gamma_n^2\|\boldsymbol{\mathcal{A}}^{-1}:\mathbf{S}_n\|^2 - 2p_e^*\gamma_n f_d\left(\boldsymbol{\mathcal{A}}^{-1}:\mathbf{S}_n\right):\mathbf{B}_n + f_d^2\|\mathbf{B}_n\|^2 - 1 = 0 \tag{41}$$

For the states at the SOM surface we have $f_d = \|\mathbf{B}_n\|^{-1}$ (32). Introducing this condition into (41) leads to

$$p_e^*\gamma_n^2\|\boldsymbol{\mathcal{A}}^{-1}:\mathbf{S}_n\|^2 - 2\gamma_n\left(\boldsymbol{\mathcal{A}}^{-1}:\mathbf{S}_n\right):\vec{\mathbf{D}}_{SOM} = 0 \tag{42}$$

where $\vec{\mathbf{D}}_{SOM}$ is the direction of the proportional stretching corresponding to the swept-out-memory conditions for a given state $\mathbf{T}_n$ (from 33):

$$\vec{\mathbf{D}}_{SOM} = -\frac{\mathbf{B}_n}{\|\mathbf{B}_n\|} \tag{43}$$

As γ_n represents the norm of $\dot{\mathbf{T}}_n$, it must be positive or null. Therefore, possible directions $\mathbf{S}_n$ must be confined in the half-space defined by

$$\left(\boldsymbol{\mathcal{A}}^{-1}:\mathbf{S}_n\right):\vec{\mathbf{D}}_{SOM} > 0 \tag{44}$$

where the plane

$$\left(\boldsymbol{\mathcal{A}}^{-1}:\mathbf{S}_n\right):\vec{\mathbf{D}}_{SOM} = 0 \tag{45}$$

represents a tangent to the normalised response envelope.

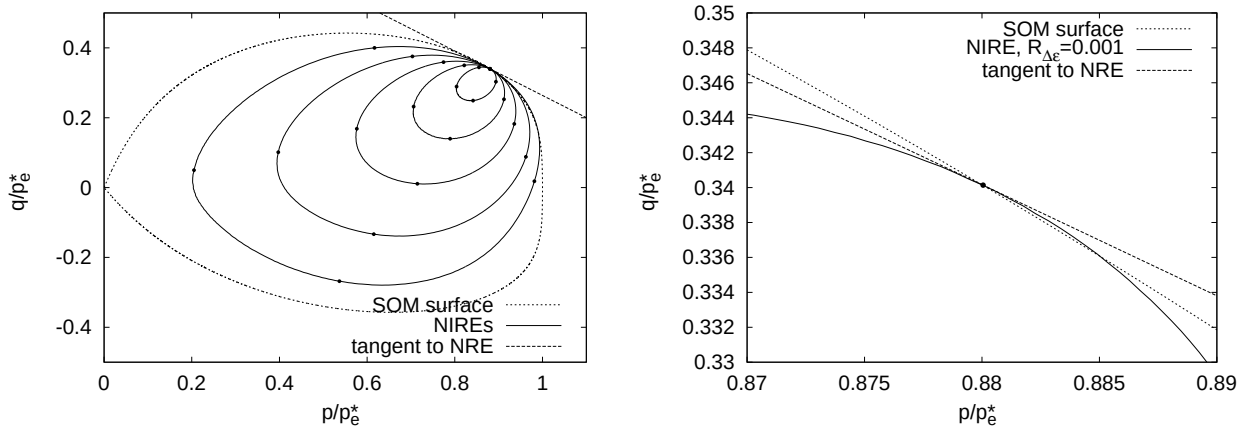

(a) (b)

Figure 7: NIREs for the initial K_{0NC} conditions. (b) provides detail of (a). NIREs are plotted for $R_{\Delta\epsilon} = 0.001, 0.0025, 0.005, 0.01, 0.02$ (a) and $R_{\Delta\epsilon} = 0.001$ (b). Points at NIREs denote compression and extension for $\mathrm{D}_{00} = \mathrm{D}_{11} = \mathrm{D}_{22}$ and $\mathrm{tr}\,\mathbf{D} = \mathbf{0}$)

Fig. 7a depicts the SOM surface, tangent to the normalised response envelope calculated according to Eq. (45) and incremental stress response envelopes (as defined in Sec. 2)

plotted in the normalised space $\mathbf{T}_n$ (normalised incremental response envelope, NIRE) for different values of $R_{\Delta\epsilon}$. Apparently, the tangent to the normalised response envelope is nearly coincident with the tangent to the SOM surface. A detailed inspection in Fig. 7b, however, reveals that the tangent to the NRE is slightly inclined with respect to the tangent to the SOM surface and therefore proves that the state boundary surface, in general, does not coincide with the swept-out-memory surface. The difference between tangents to NRE and SOM surface is even more pronounced for initial states *dry of critical* (defined by $p/p_e^* < 0.5$ in the model considered) as shown in Fig. 8[3].

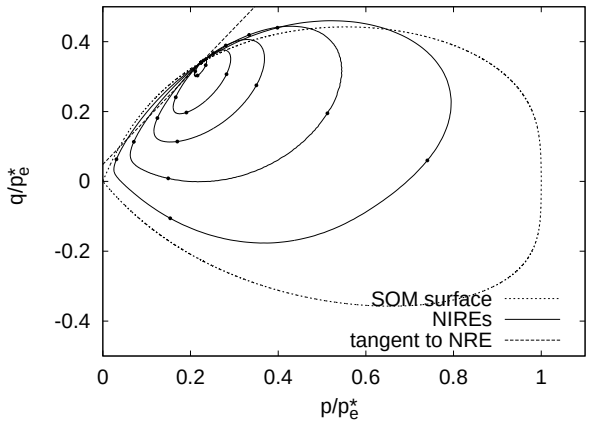

Figure 8: NIREs for the initial conditions with $p/p_e^* < 0.5$, plotted for $R_{\Delta\epsilon} = 0.001, 0.005, 0.01, 0.02, 0.035$.

Therefore, similarly to the limit and bounding surfaces of *amorphous* hypoplastic models in the stress space, the state boundary surface is located slightly outside the swept-out-memory surface. Nevertheless, taking into account uncertainties in the experimental determination of the state boundary surface, we may consider the swept-out-memory surface as a sufficient approximation of the state boundary surface. For this reason we restrict our investigations in the next sections to the SOM surface.

Figures 7 and 8 also demonstrate the asymptotic property of the considered hypoplastic model, as for large $R_{\Delta\epsilon}$ the normalised incremental response envelopes converge towards the SOM surface. The model keeps this property also for the initial states outside the SOM surface (see Fig. 9). Therefore, we see that the fact that the model allows to surpass slightly the SOM surface (SBS is located slightly outside the SOM surface) does not spoil its abilities to predict asymptotic states.

[3]In Fig. 8 normalised incremental response envelopes are cross-sected by the tangent to normalised response envelopes calculated according to (45). This fact is to be expected, as, in general, a tangent to the NRE represents a tangent to the NIRE only for $R_{\Delta\epsilon} \to 0$.

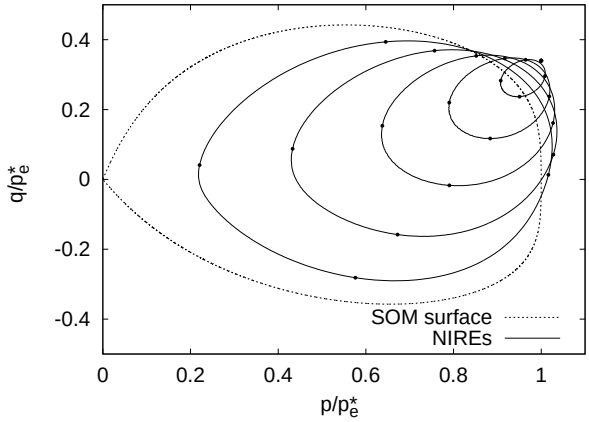

Figure 9: NIREs for the initial state outside the SOM surface. The initial state has been *imposed* and does not follow from a model prediction. NIREs are plotted for $R_{\Delta\epsilon} = 0.001, 0.0025, 0.005, 0.01, 0.02$.

7 Model performance

7.1 The influence of model parameters on the shape of the SOM surface

The SOM surface shown in Fig. 6 was found using parameters derived in [21] for London clay (with the exception of $\kappa^* = 0.014$ instead of $\kappa^* = 0.016$). They are summarised in Tab. 1.

Table 1: *Parameters for London clay used in the simulations*

φ_c [°]	λ^*	κ^*	N	r
22.6	0.11	0.014	1.375	0.4

As follows from the equations representing the SOM surface (Sec. 5), its shape is dependent on model parameters. A detailed study of Eq. (36) reveals that the parameters N and λ^* do not independently influence the shape of the SOM surface (see comments further) and the influence of the parameter r is negligible (for its reasonable values). The shape of the SOM surface is controlled by the critical state friction angle φ_c and by the ratio $(\lambda^* - \kappa^*)/(\lambda^* + \kappa^*)$ appearing in the expression for the pyknotropy factor f_d, Eq. (58).

The influence of the parameter φ_c is shown in Fig. 10a. The value of φ_c was varied in the analyses, while other parameters (Tab. 1) were kept constant. In order to normalise the response for the variation in φ_c, the SOM surface is plotted in the space $q/(Mp_e^*)$:p/p_e^* (as

suggested in [7]), where the quantity M is defined as:

$$\begin{cases} M = \dfrac{6\sin\varphi_c}{3-\sin\varphi_c} & \text{for triaxial compression} \\ M = \dfrac{6\sin\varphi_c}{3+\sin\varphi_c} & \text{for triaxial extension} \end{cases} \tag{46}$$

The influence of the ratio $(\lambda^* - \kappa^*)/(\lambda^* + \kappa^*)$ is demonstrated in Fig. 10b. The value of the parameter $\lambda^* = 0.11$ was kept constant, whereas the parameter κ^* was varied. The corresponding values of the ratio $(\lambda^* - \kappa^*)/(\lambda^* + \kappa^*)$ are also given in the figure.

Fig. 10 reveals that although the influence of the parameter φ_c and of the ratio $(\lambda^* - \kappa^*)/(\lambda^* + \kappa^*)$ on the shape of the SOM surface is significant, for reasonable values of the involved parameters the shape remains close to the one predicted by the Modified Cam clay model. Only for low values of the ratio $(\lambda^* - \kappa^*)/(\lambda^* + \kappa^*)$ (large ratio κ^*/λ^*, i.e. soft response in isotropic unloading), the SOM surface becomes non-convex in the vicinity of isotropic stress states[4].

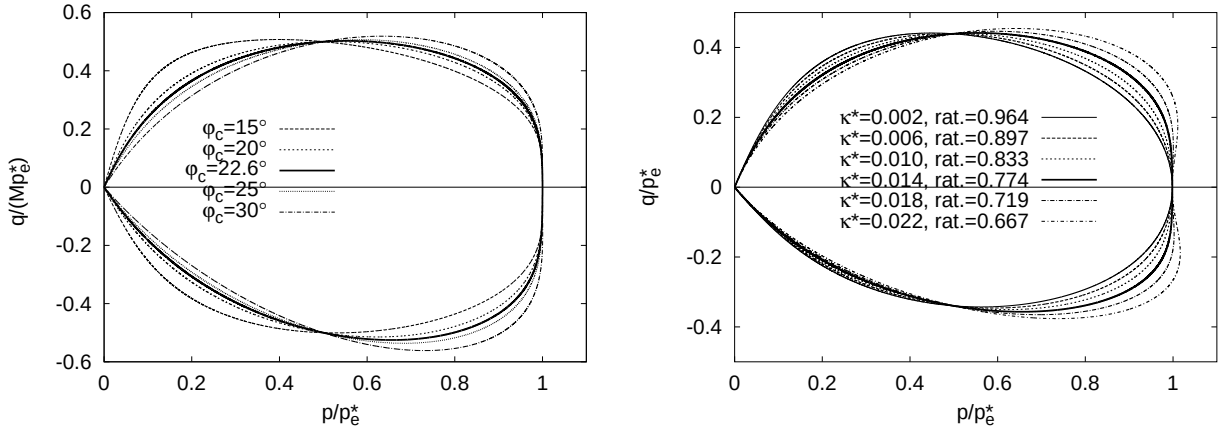

Figure 10: The influence of (a) the parameter φ_c and (b) of the ratio $(\lambda^* - \kappa^*)/(\lambda^* + \kappa^*)$ on the shape of the SOM surface

7.2 K_0 normally compressed conditions

Finally, the equations for swept-out-memory conditions are applied in a study of the influence of model parameters on K_0 conditions in the normally compressed state (K_{0NC}), see Fig. 11.

[4]The issue of convexity of a limit surface in the normalised plane is of relevance in the theory of plasticity, where the convexity of the yield surface is crucial in order to properly define loading/unloading conditions. In hypoplasticity, whether a non-convex SOM surface is acceptable or not can be judged only with reference to available experimental data.

The parameter φ_c and the ratio $(\lambda^* - \kappa^*)/(\lambda^* + \kappa^*)$ were varied as in Sec. 7.1. Predictions of K_{0NC} by the hypoplastic model are compared with Jáky's [16] equation

$$K_{0NC} = 1 - \sin \varphi_c \tag{47}$$

As demonstrated for example in [25], Eq. (47) is suitable for fine-grained soils. Predictions

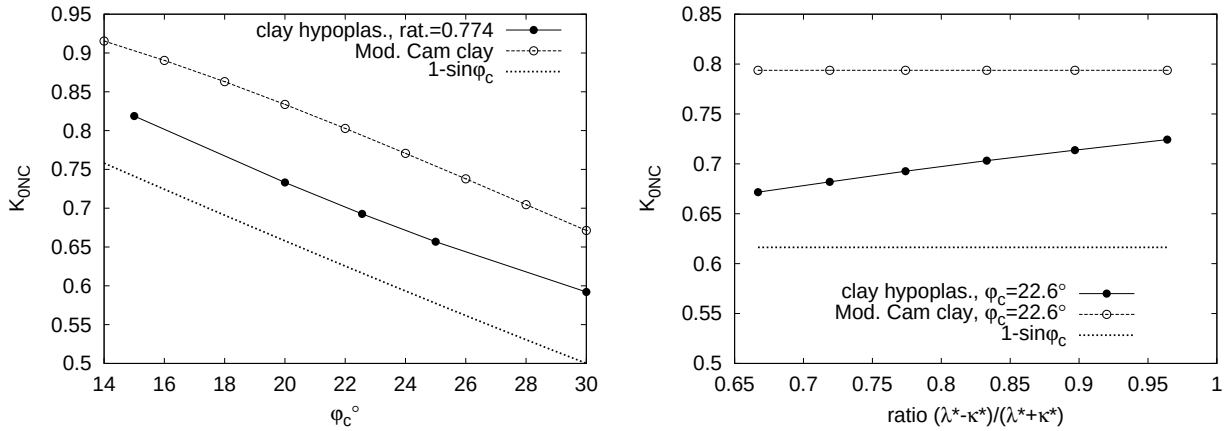

(a) (b)

Figure 11: K_{0NC} conditions predicted by the considered model, compared to Jáky's [16] formula and predictions by the Modified Cam clay model [29].

by the Modified Cam clay model [29] are also included in Fig. 11. In the calculation with the Modified Cam clay model, the influence of elastic strain increments, which are at the yield surface negligible compared to the plastic strain increments, is omitted. Consequently,

$$K_{0NC} = \frac{3 - \eta}{3 + 2\eta} \tag{48}$$

for the Modified Cam clay model, with

$$\eta = \frac{\sqrt{9 + 4M^2} - 3}{2} \quad \text{and} \quad M = \frac{6 \sin \varphi_c}{3 - \sin \varphi_c} \tag{49}$$

It can be seen in Fig. 11 that the considered hypoplastic model predicts correctly the trend of decreasing K_{0NC} with increasing φ_c. Although the hypoplastic model overpredicts K_{0NC} as compared to Eq. (47), its predictions are still significantly closer to Eq. (47) than the predictions by the Modified Cam clay model.

Further discussion on the direction of stretching $\vec{\mathbf{D}}$ at SOM conditions with respect to the corresponding $\vec{\mathbf{T}}$, as well as on the SOM conditions predicted by different *endomorphous* hypoplastic models, may be found in [22].

8 Concluding remarks

The present paper studied if the hypoplastic model for clays [21] predicts, as a by–product of the constitutive formulation, the existence of the state boundary surface, which may be seen as a key characteristics of the behaviour of fine–grained soils.

It has been shown that for the given model it is possible to derive an explicit formulation for the so-called swept-out-memory surface, which may be defined as an envelope of asymptotic (swept-out-memory) states in the stress-void ratio space. The concept of the normalised incremental stress response envelopes and the derivation of the tangent to the normalised rate response envelopes was subsequently used to demonstrate that the swept-out-memory surface is a close approximation of the state boundary surface, although, in general, they do not coincide. It has been shown that there is a direct parallel between the swept-out-memory and the state boundary surfaces defined in the stress-void ratio space for *endomorphous* hypoplastic models, and limit and bounding surfaces defined in the stress space for *amorphous* hypoplastic models.

Finally the influence of the constitutive parameters on the shape of the swept-out-memory surface has been studied by means of a parametric study. For parameters suitable for fine-grained soils, the considered hypoplastic model predicts a swept-out-memory surface of a similar shape to the state boundary surface of the Modified Cam clay model. However, the K_0 values at normally compressed states are better predicted by the hypoplastic model than by the Modified Cam clay model.

A study of the shape of the SOM surface (Sec. 7) and invertibility condition of $\boldsymbol{\mathcal{A}}$ (Appendix B) reveal limitation of the hypoplastic model for clays, which does not perform correctly for soils very soft in isotropic unloading. As a *very rough* guide, condition $\kappa^* < \lambda^*/4$ should be satisfied when using model [21]. More precise investigation requires to plot the SOM surface and to ensure that the condition (66) is not satisfied.

9 Acknowledgement

The first author gratefully acknowledges the financial support by the research grants SSPI-CT-2003-501837-NOAH'S ARK under the EC 6^{th} FP and GACR 103/04/0672. Valuable remarks by the anonymous journal reviewers are highly appreciated.

Appendix A

The mathematical structure of the hypoplastic model for clays is discussed in detail in [21]. The constitutive equation in rate form reads:

$$\mathring{\mathbf{T}} = f_s \boldsymbol{\mathcal{L}} : \mathbf{D} + f_s f_d \mathbf{N} \|\mathbf{D}\| \tag{50}$$

where:

$$\boldsymbol{\mathcal{L}} = 3\left(c_1 \boldsymbol{\mathcal{I}} + c_2 a^2 \hat{\mathbf{T}} \otimes \hat{\mathbf{T}}\right) \qquad \mathbf{N} = \boldsymbol{\mathcal{L}} : \left(-Y \frac{\mathbf{m}}{\|\mathbf{m}\|}\right) \qquad \hat{\mathbf{T}} := \frac{\mathbf{T}}{\operatorname{tr} \mathbf{T}} \tag{51}$$

$\mathbf{1}$ is the second–order identity tensor and $\boldsymbol{\mathcal{I}}$ is the fourth–order identity tensor, with components:

$$(\mathcal{I})_{ijkl} := \frac{1}{2}\left(1_{ik}1_{jl} + 1_{il}1_{jk}\right) \tag{52}$$

In eq. (50), the functions $f_s(\operatorname{tr} \mathbf{T})$ (*barotropy* factor) and $f_d(\operatorname{tr} \mathbf{T}, e)$ (*pyknotropy* factor) are given by:

$$f_s = -\frac{\operatorname{tr}\mathbf{T}}{\lambda^*}\left(3 + a^2 - 2^\alpha a\sqrt{3}\right)^{-1} \qquad f_d = \left[-\frac{2\operatorname{tr}\mathbf{T}}{3p_r}\exp\left(\frac{\ln(1+e) - N}{\lambda^*}\right)\right]^\alpha \tag{53}$$

where p_r is the reference stress 1 kPa. The scalar function Y and the second–order tensor $\mathbf{m}$ appearing in Eq. (51) are given, respectively, by:

$$Y = \left(\frac{\sqrt{3}a}{3 + a^2} - 1\right)\frac{(I_1 I_2 + 9I_3)\left(1 - \sin^2\varphi_c\right)}{8I_3 \sin^2\varphi_c} + \frac{\sqrt{3}a}{3 + a^2} \tag{54}$$

in which:

$$I_1 := \operatorname{tr}\mathbf{T} \qquad I_2 := \frac{1}{2}\left[\mathbf{T} : \mathbf{T} - (I_1)^2\right] \qquad I_3 := \det \mathbf{T}$$

and

$$\mathbf{m} = -\frac{a}{F}\left[\hat{\mathbf{T}} + \hat{\mathbf{T}}^* - \frac{\hat{\mathbf{T}}}{3}\left(\frac{6\ \hat{\mathbf{T}} : \hat{\mathbf{T}} - 1}{(F/a)^2 + \hat{\mathbf{T}} : \hat{\mathbf{T}}}\right)\right] \tag{55}$$

in which:

$$\hat{\mathbf{T}}^* = \hat{\mathbf{T}} - \frac{\mathbf{1}}{3} \qquad F = \sqrt{\frac{1}{8}\tan^2\psi + \frac{2 - \tan^2\psi}{2 + \sqrt{2}\tan\psi\cos 3\theta}} - \frac{1}{2\sqrt{2}}\tan\psi \tag{56}$$

$$\tan\psi = \sqrt{3}\|\hat{\mathbf{T}}^*\| \qquad \cos 3\theta = -\sqrt{6}\frac{\operatorname{tr}\left(\hat{\mathbf{T}}^* \cdot \hat{\mathbf{T}}^* \cdot \hat{\mathbf{T}}^*\right)}{\left(\hat{\mathbf{T}}^* : \hat{\mathbf{T}}^*\right)^{3/2}} \tag{57}$$

Finally, the scalars a, α, c_1 and c_2 appearing in eqs. (51)–(55), are given as functions of the material parameters φ_c, λ^*, κ^* and r by the following relations:

$$a = \frac{\sqrt{3}\,(3-\sin\varphi_c)}{2\sqrt{2}\sin\varphi_c} \qquad \alpha = \frac{1}{\ln 2}\,\ln\left[\frac{\lambda^*-\kappa^*}{\lambda^*+\kappa^*}\left(\frac{3+a^2}{a\sqrt{3}}\right)\right] \tag{58}$$

$$c_1 = \frac{2\left(3+a^2-2^\alpha a\sqrt{3}\right)}{9r} \qquad c_2 = 1+(1-c_1)\frac{3}{a^2} \tag{59}$$

The model requires five constitutive parameters, namely φ_c, λ^*, κ^*, N and r, state is characterised by the Cauchy stress $\mathbf{T}$ and void ratio e.

Appendix B

In this Appendix invertibility of the tensor $\boldsymbol{\mathcal{A}}$ is discussed. Eq. (29) can be written with help of Eqs. (51) and (53) as

$$\begin{aligned}\boldsymbol{\mathcal{A}} &= -\frac{\mathrm{tr}\mathbf{T}}{\lambda^*}\left[f_s^* 3c_1\boldsymbol{\mathcal{I}} - \hat{\mathbf{T}}\otimes\mathbf{1} + f_s^* 3c_2 a^2\hat{\mathbf{T}}\otimes\hat{\mathbf{T}}\right]\\ &= -\frac{\mathrm{tr}\mathbf{T}}{\lambda^*}\left[f_s^* 3c_1\boldsymbol{\mathcal{I}} - \hat{\mathbf{T}}\otimes\mathbf{1} + f_s^*\left[3a^2+9(1-c_1)\right]\hat{\mathbf{T}}\otimes\hat{\mathbf{T}}\right]\end{aligned} \tag{60}$$

with

$$f_s^* = \left(3+a^2-2^\alpha a\sqrt{3}\right)^{-1} > 0 \tag{61}$$

for any realistic values of a and α. Eq. (60) can be also written as

$$\boldsymbol{\mathcal{A}} = -\frac{\mathrm{tr}\mathbf{T}}{\lambda^*}\left[C_1\boldsymbol{\mathcal{I}} - \hat{\mathbf{T}}\otimes\mathbf{1} + C_2\hat{\mathbf{T}}\otimes\hat{\mathbf{T}}\right] \tag{62}$$

with C_1, C_2 being scalar constants calculated from model parameters.

$$C_1 = \frac{2}{3r} \quad \text{and} \quad C_2 = \frac{2a^2+6(1-c_1)}{3rc_1} \tag{63}$$

To study the invertibility condition of $\boldsymbol{\mathcal{A}}$, it is sufficient to consider tensor $\boldsymbol{\mathcal{A}}^* = -\lambda^*\boldsymbol{\mathcal{A}}/\mathrm{tr}\mathbf{T}$ (only $\mathrm{tr}\mathbf{T} < 0$ is allowed). In the principal stress components the determinant of $\boldsymbol{\mathcal{A}}^*$ reads

$$\det\boldsymbol{\mathcal{A}}^* = C_1^3 - C_1^2\left[(\hat{T}_1+\hat{T}_2+\hat{T}_3) - C_2(\hat{T}_1^2+\hat{T}_2^2+\hat{T}_3^2)\right] \tag{64}$$

Inversion of the tensor $\boldsymbol{\mathcal{A}}$ is possible if $\det\boldsymbol{\mathcal{A}}^* \neq 0$. Because $C_1 \neq 0$ and $\hat{T}_1+\hat{T}_2+\hat{T}_3 = 1$, this condition reads

$$C_1 - 1 + C_2(\hat{T}_1^2+\hat{T}_2^2+\hat{T}_3^2) \neq 0 \tag{65}$$

Taking into account definitions of scalars C_1 and C_2 (63) and the fact that for compressive stresses $1/3 < (\hat{T}_1^2 + \hat{T}_2^2 + \hat{T}_3^2) < 1$, we find that the invertibility of $\boldsymbol{\mathcal{A}}$ is *not* guaranteed if

$$\frac{1}{3}\left[\frac{2a^2 + 6(1 - c_1)}{c_1}\right] < (3r - 2) < \frac{2a^2 + 6(1 - c_1)}{c_1} \tag{66}$$

A detailed study of the condition (66) reveals that for reasonable values of material parameters the tensor $\boldsymbol{\mathcal{A}}$ is invertible. For example for London clay parameters (Tab. 1) the condition (66) reads $3.31 < -0.8 < 9.94$. The invertibility of $\boldsymbol{\mathcal{A}}$ may not be guaranteed for unrealistically low values of the ratio $(\lambda^* - \kappa^*)/(\lambda^* + \kappa^*)$.

References

[1] E. Bauer. Modelling of critical stress in hypoplasticity. In *NUMOG V*, pages 15–20, Davos, 1995. Balkema.

[2] R. Butterfield. A natural compression law for soils. *Géotechnique*, 29(4):469–480, 1979.

[3] F. Calvetti, C. Tamagnini, and G. Viggiani. On the incremental behaviour of granular soils. In *NUMOG VIII*, pages 3–9. Swets & Zeitlinger, 2002.

[4] R. Chambon. Une classe de lois de comportement incrémentalement nonlináires pour les sols non visqueux, résolution de quelques problèmes de cohérence. *C. R. Acad. Sci.*, 308(II):1571–1576, 1989.

[5] R. Chambon, J. Desrues, W. Hammad, and R. Charlier. CLoE, a new rate–type constitutive model for geomaterials. Theoretical basis and implementation. *International Journal for Numerical and Analytical Methods in Geomechanics*, 18:253–278, 1994.

[6] D. Costanzo, G. Viggiani, and C. Tamagnini. Directional response of a reconstituted fine grained soil. Part I: Experimental investigation. *International Journal for Numerical and Analytical Methods in Geomechanics (submitted for publication)*, 2005.

[7] F. Cotecchia and J. Chandler. A general framework for the mechanical behaviour of clays. *Géotechnique*, 50(4):431–447, 2000.

[8] R. Cudmani and V. A. Osinov. The cavity expansion problem for the interpretation of cone penetration and pressuremeter tests. *Canadian Geotechnical Journal*, 38:622–638, 2001.

[9] Y. F. Daffalias. Bounding surface plasticity. I: Mathematical foundation and hypoplasticity. *Journal of Engineering Mechanics ASCE*, 112(9):966–987, 1986.

[10] G. Gudehus. A comparison of some constitutive laws for soils under radially symmetric loading and unloading. In *Proc. 3rd Int. Conf. on Numerical Methods in Geomechanics*, pages 1309–1323. Aachen, 1979.

[11] G. Gudehus. Attractors for granular storage and flow. In *3rd European Symposium – Storage and Flow of Particulate Solids, Paper for the conf. 'Partec 95'*, pages 333–345, 1995.

[12] G. Gudehus. A comprehensive constitutive equation for granular materials. *Soils and Foundations*, 36(1):1–12, 1996.

[13] G. Gudehus. A visco-hypoplastic constitutive relation for soft soils. *Soils and Foundations*, 44(4):11–25, 2004.

[14] G. Gudehus, M. Goldscheider, and H. Winter. Mechanical properties of sand and clay and numerical intergration methods: some sources of errors and bounds of accuracy. In G. Gudehus, editor, *Finite Elements in Geomechanics*, pages 121–150. Wiley, 1977.

[15] I. Herle and D. Kolymbas. Hypoplasticity for soils with low friction angles. *Computers and Geotechnics*, 31(5):365–373, 2004.

[16] J. Jáky. The coefficient of earth pressure at rest. *Journal for Society of Hungarian Architects and Engineers*, pages 355–357, 1944.

[17] C. Karcher. Tagebaubedingte Deformationen im Lockergestein. Veröffentlichungen des Institutes für Bodenmechanik und Felsmechanik der Universität Fridericiana in Karlsruhe, 2003. Heft 160.

[18] D. Kolymbas. Computer-aided design of constitutive laws. *International Journal for Numerical and Analytical Methods in Geomechanics*, 15:593–604, 1991.

[19] D. Kolymbas. An outline of hypoplasticity. *Archive of Applied Mechanics*, 61:143–151, 1991.

[20] J. Lanier, D. Caillerie, R. Chambon, G. Viggiani, P. Bésuelle, and J. Desrues. A general formulation of hypoplasticity. *International Journal for Numerical and Analytical Methods in Geomechanics*, 28:1461–1478, 2004.

[21] D. Mašín. A hypoplastic constitutive model for clays. *International Journal for Numerical and Analytical Methods in Geomechanics*, 29(4):311–336, 2005.

[22] D. Mašín and I. Herle. State boundary surface in hypoplasticity. In *Proc. Int. workshop Modern trends in geomechanics (in print)*. Vienna, Austria, 2005.

[23] D. Mašín, C. Tamagnini, G. Viggiani, and D. Costanzo. Directional response of a reconstituted fine grained soil. Part II: Performance of different constitutive models. *International Journal for Numerical and Analytical Methods in Geomechanics (submitted for publication)*, 2005.

[24] P.-M. Mayer. Verformungen und Spannungsänderungen im Boden durch Schlitzwandherstellung und Baugrubenaushub. Veröffentlichungen des Institutes für Bodenmechanik und Felsmechanik der Universität Fridericiana in Karlsruhe, 2000. Heft 151.

[25] P. W. Mayne and F. H. Kulhawy. K_0–OCR relationships in soil. In *Proc. ASCE J. Geotech. Eng. Div.*, volume 108, pages 851–872, 1982.

[26] A. Niemunis. A visco-plastic model for clay and its FE implementation. In E. Dembicki, W. Cichy, and L. Balachowski, editors, *Recent results in mechanics of soils and rocks.*, pages 151–162. TU Gdańsk, 1996.

[27] A. Niemunis. *Extended hypoplastic models for soils*. Habilitation thesis, Ruhr-University, Bochum, 2002.

[28] K. Nübel and R. Cudmani. Examples of finite element calculations with the hypoplastic law. In D. Kolymbas, editor, *Constitutive Modelling of Granular Materials*, pages 523–538. Springer, 2000.

[29] K. H. Roscoe and J. B. Burland. On the generalised stress-strain behaviour of wet clay. In J. Heyman and F. A. Leckie, editors, *Engineering Plasticity*, pages 535–609. Cambridge: Cambridge Univesrity Press, 1968.

[30] P. Royis and T. Doanh. Theoretical analysis of strain response envelopes using incrementally non-linear constitutive equations. *International Journal for Numerical and Analytical Methods in Geomechanics*, 22(2):97–132, 1998.

[31] A. N. Schofield and C. P. Wroth. *Critical state soil mechanics*. McGraw-Hill Book Co., London, 1968.

[32] S. E. Stallebrass and R. N. Taylor. Prediction of ground movements in overconsolidated clay. *Géotechnique*, 47(2):235–253, 1997.

[33] C. Tamagnini, D. Mašín, G. Viggiani, and D. Costanzo. An evaluation of different constitutive models to predict the directional response of a reconstituted fine-grained soils. In *Proc. Int. workshop Modern trends in geomechanics (in print)*. Vienna, Austria, 2005.

[34] C. Tamagnini, G. Viggiani, and R. Chambon. A review of two different approaches to hypoplasticity. In D. Kolymbas, editor, *Constitutive modelling of granular materials*, pages 107–144. Springer, 1999, 1999.

[35] C. Tamagnini, G. Viggiani, R. Chambon, and J. Desrues. Evaluation of different strategies for the integration of hypoplastic constitutive equations. *Mechanics of Cohesive-Frictional Materials*, 5:263–289, 2000.

[36] J. Tejchman and I. Herle. A "class A" prediction of the bearing capacity of plane strain footings on sand. *Soils and Foundations*, 39(5):47–60, 1999.

[37] P. A. von Wolffersdorff. A hypoplastic relation for granular materials with a predefined limit state surface. *Mechanics of Cohesive-Frictional Materials*, 1:251–271, 1996.

[38] W. Wu. *Hypoplastizität als mathematisches Modell zum mechanischen Verhalten granularer Stoffe*. PhD thesis, Karlsruhe University, Germany, 1992.

[39] W. Wu and A. Niemunis. Beyond failure in granular materials. *International Journal for Numerical and Analytical Methods in Geomechanics*, 21:153–175, 1997.